JOURNAL OF VIROLOGY, Mar. 2006, p. 2267–2279 Vol. 80, No. 5
0022-538X/06/$08.00+0 doi:10.1128/JVI.80.5.2267–2279.2006

A Single Intranasal Inoculation with a Paramyxovirus-Vectored Vaccine Protects Guinea Pigs against a Lethal-Dose Ebola Virus Challenge

Alexander Bukreyev,[1]* Lijuan Yang,[1] Sherif R. Zaki,[2] Wun-Ju Shieh,[2] Pierre E. Rollin,[2] Brian R. Murphy,[1] Peter L. Collins,[1] and Anthony Sanchez[2]

National Institute of Allergy and Infectious Diseases, National Institutes of Health, Bethesda, Maryland,[1] and National Center for Infectious Diseases, Centers for Disease Control and Prevention, Atlanta, Georgia[2]

Received 23 August 2005/Accepted 9 December 2005

To determine whether intranasal inoculation with a paramyxovirus-vectored vaccine can induce protective immunity against Ebola virus (EV), recombinant human parainfluenza virus type 3 (HPIV3) was modified to express either the EV structural glycoprotein (GP) by itself (HPIV3/EboGP) or together with the EV nucleoprotein (NP) (HPIV3/EboGP-NP). Expression of EV GP by these recombinant viruses resulted in its efficient incorporation into virus particles and increased cytopathic effect in Vero cells. HPIV3/EboGP was 100-fold more efficiently neutralized by antibodies to EV than by antibodies to HPIV3. Guinea pigs infected with a single intranasal inoculation of $10^{5.3}$ PFU of HPIV3/EboGP or HPIV3/EboGP-NP showed no apparent signs of disease yet developed a strong humoral response specific to the EV proteins. When these animals were challenged with an intraperitoneal injection of 10^3 PFU of EV, there were no outward signs of disease, no viremia or detectable EV antigen in the blood, and no evidence of infection in the spleen, liver, and lungs. In contrast, all of the control animals died or developed severe EV disease following challenge. The highly effective immunity achieved with a single vaccine dose suggests that intranasal immunization with live vectored vaccines based on recombinant respiratory viruses may be an advantageous approach to inducing protective responses against severe systemic infections, such as those caused by hemorrhagic fever agents.

Ebola virus (EV) is one of the most pathogenic viruses known; it and another highly pathogenic agent, Marburg virus, constitute the family *Filoviridae* (Order *Mononegavirales*). It causes severe hemorrhagic fever in humans, with a mortality rate of up to 88%, and lacks an approved vaccine or antiviral therapy. The virus is easily transmitted from acutely infected humans and animals by body fluids coming in contact with mucosal surfaces or wounds, and safe handling of infectious virus requires biosafety level 4 (BSL-4) containment (19, 28, 38). Following the first recorded outbreak in 1976, the Zaire and Sudan species of EV have caused sporadic outbreaks of human disease in Central Africa, but in the past decade the incidence has increased to once every few years (33) and also has involved endangered populations of great apes (37). The source of these outbreaks is unknown, as the ecology (natural host) of filoviruses remains a mystery (33).

Severe EV disease is characterized by virus replication throughout the body, particularly in the spleen and liver, resulting in a high virus load and prominent antigenemia (19, 28, 38). This widespread replication is facilitated by the expression of viral genes that lead to immune evasion by blocking interferon pathways (3), inducing apoptosis in lymphocytes (indirectly) (1, 2, 17), and impairing maturation of antigen-presenting cells (5, 6, 18, 29). The genome of EV is a single-stranded RNA of negative polarity of approximately 19 kb in length with a gene order of 3′-NP-VP35(or P)-VP40(or M)-GP-VP30-VP24-L-5′ (40). Each gene is transcribed into a monocistronic mRNA (39). The major surface glycoprotein (GP) is synthesized as the full-length 676-amino-acid type I membrane-anchored protein and as a C-terminally truncated 364-amino-acid secreted version (sGP). Full-length GP is expressed from a GP mRNA that is modified by cotranscriptional editing, involving the insertion of a single A residue at a specific sequence motif midway along the open reading frame (ORF), whereas sGP is encoded by the unedited transcript (41, 50). Full-length GP undergoes posttranslational proteolytic cleavage, at a multibasic amino acid motif located at positions 497 to 501 of the ORF, into two disulfide-linked fragments, GP1 and GP2 (52). Expression of GP has been shown to be associated with enhanced cytopathic effect (CPE) in cell culture and is thought to cause a vascular cytotoxicity during the acute phase of EV infection (46, 55). However, another study, involving cynomolgus monkeys, demonstrated that EV infection does not extensively disrupt the vascular endothelium (22).

Attempts to develop a protective vaccine against EV disease have had limited success (reviewed in references 14 and 20). Several recombinant candidate vaccines have shown promising results in rodent models yet have failed to provide adequate protection when tested in nonhuman primates, which present a more stringent model due to their extreme susceptibility to EV infection. Recently, however, two vaccines were found to be effective in primate models: one involves a replication-deficient adenovirus expressing EV GP or GP together with the major nucleoprotein (NP), and the other involves a replication-competent vesicular stomatitis virus expressing GP in the place of its own G glycoprotein (24, 45, 47). Intramuscular injection of these viruses protected cynomolgus macaques against subsequent challenge with EV.

Mucosal immunization against EV and other hemorrhagic fevers has not been explored, yet immunization through the

* Corresponding author. Mailing address: LID, NIAID, NIH, 50 South Drive, Rm. 6505, Bethesda, MD 20892-8007. Phone: (301) 594-1854. Fax: (301) 496-8312. E-mail: abukreyev@niaid.nih.gov.

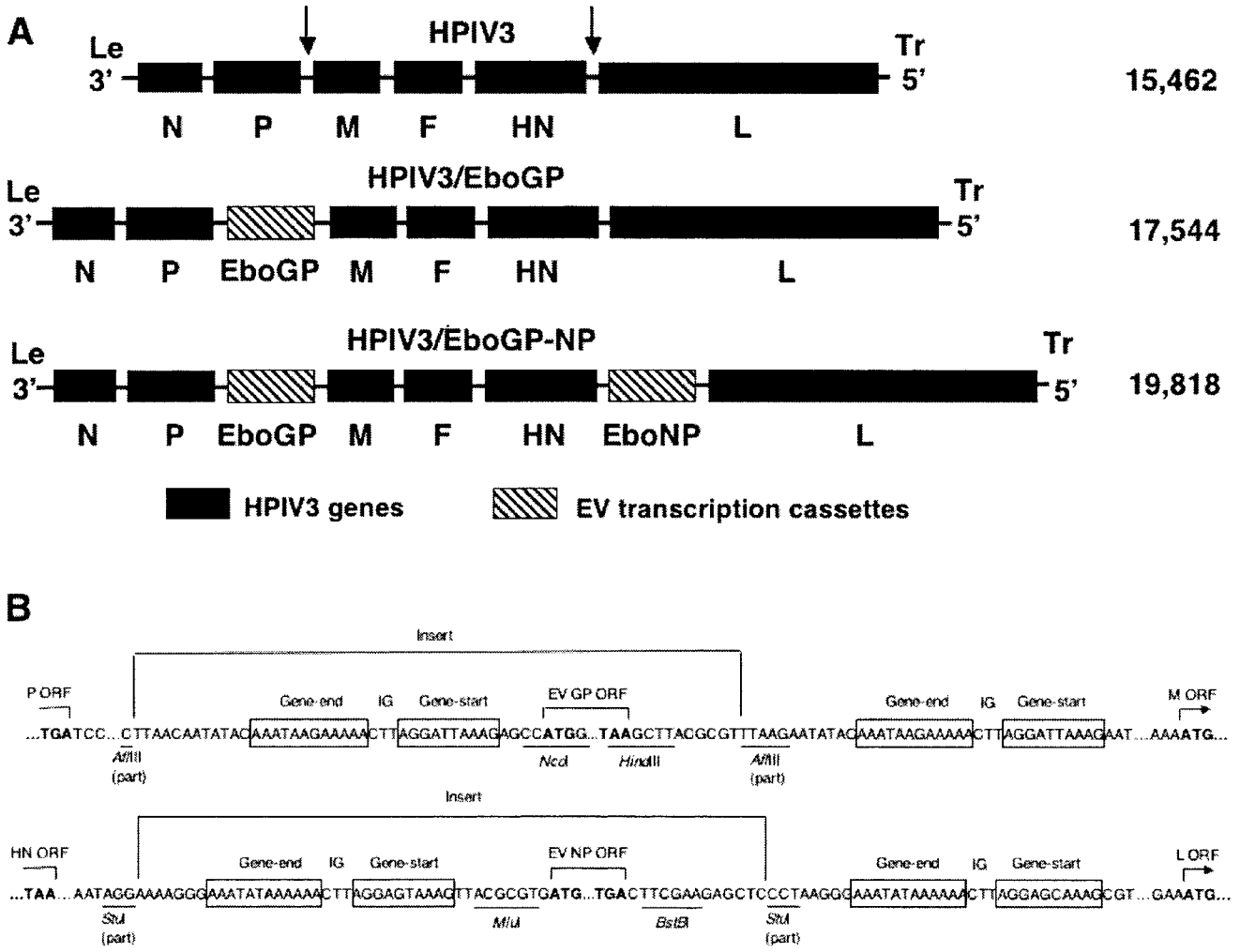

FIG. 1. Genome structures of recombinant HPIV3s expressing EV GP and NP. (A) Schematic diagrams of the genome of the HPIV3 vector, with insertion sites indicated by arrows (top) and HPIV3 vectors containing a transcription cassette encoding EV GP (middle) or two separate cassettes encoding GP and NP (bottom). The genomic length of each construct (in nucleotides) is indicated to the right. (B) Sequences flanking the EV GP (top) and NP (bottom) ORFs in the HPIV3 genome, shown in antigenomic or positive sense. The boundaries of the GP and NP inserts are indicated. HPIV3-specific gene start and gene end transcriptional signals are boxed, the three-nucleotide-long intergenic sequence is designated IG, and the initiation and stop codons of the GP and NP ORFs are in boldface, with the remainder of each ORF indicated by three dots. Restriction endonuclease sites used for cloning are indicated below their underlined sequences.

respiratory tract has been shown to be a highly effective means of inducing both local and systemic immune responses against respiratory viral infections. A live attenuated intranasal influenza vaccine has recently become commercially available (reviewed in reference 25), and several live attenuated vaccines against human respiratory syncytial virus (RSV) and human parainfluenza viruses (HPIVs) are currently in clinical trials (30). In the case of EV, the respiratory tract appears to be a possible portal of entry for EV infection (23, 42), and direct stimulation of local immunity would be important in cases where this occurs. In this study, the efficacy of intranasal mucosal immunization against parenterally administered EV challenge was evaluated with a guinea pig model using HPIV serotype 3 (HPIV3) as a vector for the expression of EV GP and NP. This report shows that a single intranasal administration of this viral vector is capable of inducing highly effective immunity, suggesting that paramyxoviruses have potential as vectors for vaccinating humans. Although common human pathogens such as HPIV3 probably would not be effective as vectors in the adult population due to the prevalence of antibodies against the vector, other nonhuman paramyxoviruses are being developed as vectors for human use (8).

MATERIALS AND METHODS

Cells, viruses, and animals. Monkey kidney LLC-MK2, Vero, and Vero E6 cells (American Type Culture Collection [ATCC], Manassas, VA) were used for growth and quantitation of HPIV3 strain JS and its derivatives (HPIV3/EboGP and HPIV3/EboGP-NP), and Vero E6 cells were used for EV. A guinea pig-adapted EV (Zaire species, 1976 Mayinga strain) was used to challenge immunized animals (12). This virus is highly virulent for guinea pigs. In a previous study, it was found that 1 PFU contains 400 50% lethal doses, and all infections were lethal (unpublished data). All experiments involving infectious EV particles were performed under BSL-4 containment at the CDC, Atlanta, GA. Most of the experiments involving infectious HPIV3 bearing EV proteins were performed under BSL-3 containment at the NIH, Bethesda, MD, or under BSL-4 contain-

ment at the CDC, Atlanta, GA. However, when it was observed that HPIV3 expressing EV proteins did not cause illness in guinea pigs, a limited number of in vitro experiments subsequently were performed at BSL-2 using face shields and under conditions of increased infection control. These guidelines were approved by biosafety committees at the CDC and the NIH.

Construction of cDNAs and production of recombinant viruses. A cDNA encoding the HPIV3 antigenome was modified by the insertion, between the P and M genes, of the EV GP ORF under the control of a set of HPIV3 gene start and gene end signals (Fig. 1A). Specifically, a cDNA containing the full-length, edited version of the EV GP ORF of the Zaire species, Mayinga strain, was amplified by PCR from a cloned cDNA. The forward primer was GTATCAT*CC ATGG*GCGTTACAGGAATATT (the beginning of the ORF is underlined, and an NcoI site is italicized), and the reverse primer was TACACTT*AAGCTT*AA AAGACAAATTTGCATAT (the end of ORF and the stop codon are underlined, and a HindIII site is italicized). The GP PCR product was digested with NcoI and HindIII and cloned into the NcoI-HindIII window of the plasmid pUC(GE/GS)$_{P\text{-}M}$ (44). This placed the GP ORF downstream of a copy of an HPIV3 gene junction (containing a set of HPIV3 gene end, intergenic, and gene start sequences) and flanked by AflII sites (Fig. 1B). The AflII fragment was transferred by several cloning steps into the full-length HPIV3 antigenomic cDNA (Fig. 1B) to yield the plasmid pHPIV3/EboGP. A second construct was made in which pHPIV3/EboGP was modified by the additional insertion, between the HN and L genes, of the EV NP ORF under the control of a set of HPIV3 gene start and gene end signals (Fig. 1A and B). Specifically, a cDNA containing the NP ORF of the same EV strain was amplified by PCR from a cDNA clone by using the forward primer TACACTT*ACGCGT*GATGGATT CTCGTCCTCAGAA (the beginning of the ORF is underlined, and an MluI site is italicized) and the reverse primer TACACTTT*TCGAA*GTCACTGATGA TGTTGCAGGA (the end of the ORF and the stop codon are underlined, and a BstBI site is italicized). The PCR product was digested with MluI and BstBI and cloned into the MluI-BstBI window of the plasmid pHPIV3(XhoI-SphI)StuI (43). This placed the NP ORF downstream of a copy of an HPIV3 gene junction and flanked by StuI sites. The StuI fragment was transferred by several cloning steps into the full-length HPIV3 antigenomic cDNA (Fig. 1B) to yield the plasmid pHPIV3/EboGP-NP. The GP and NP inserts in both constructs were designed to comply with the rule of six and to have the inserted genes positioned so as to initiate appropriately at the first position of their respective hexamers without disturbing the start positions of the remaining genes (26).

Two recombinant viruses, HPIV3/EboGP and HPIV3/EboGP-NP, were generated by transfection of the respective antigenomic plasmid into BHK-21 cells constitutively expressing the T7 polymerase (7) together with the N, P, and L support plasmids (13). The viruses were propagated by two passages in LLC-MK2 cells. The genomic regions containing the GP and NP inserts were amplified by reverse transcription-PCR and analyzed by sequencing the uncloned PCR product. As described in Results, the first set of recovered viruses was found to have nucleotide substitutions or deletions in a run of eight A residues that constitutes part of the editing site of the GP ORF (Fig. 2). Therefore, the GP cDNA was modified so that two of the A residues in this run were changed to G residues without changing amino acid coding. This was done by site-directed mutagenesis of a cDNA containing the full-length, edited version of the EV GP ORF using the QuikChange II kit (Stratagene, La Jolla, CA), the forward primer GGCCTTCTGGGAAACTAAGAAGAACCTCACTAGAAAAATTCG, and the reverse primer CGAATTTTTCTAGTGAGGTTCTTCTTAGTTTCCCAGAAG GCC (the mutagenized nucleotide residues are underlined) according to the manufacturer's recommendations. The modified GP cDNA was used to remake the HPIV3/EboGP and HPIV3/EboGP-NP viruses by the same strategy as described above. Mutations were not observed in the GP or NP ORFs in the viruses recovered using these further-modified plasmids.

Analysis of viral proteins. LLC-MK2 cells were infected with HPIV3, HPIV3/EboGP, or HPIV3/EboGP-NP at an input multiplicity of infection (MOI) of 0.2 PFU per cell. At 24 h postinfection, lysates were prepared for the analysis of cell-associated proteins. For the analysis of virion-associated proteins, virus particles were isolated as previously described (9) from the supernatant of cells infected with HPIV3 or HPIV3/EboGP. As a control, medium from uninfected cells was processed in parallel. Briefly, the medium was clarified by low-speed centrifugation, layered onto a 30% to 60% (wt/vol) sucrose gradient, and centrifuged at 130,000 × *g* for 90 min at 4°C, and the resulting band of virus particles was isolated. Proteins from lysates of cells or purified virus preparations were electrophoretically separated under denaturing and reducing conditions in 4 to 12% or 10% bis-Tris acrylamide gradient gels (NuPage protein electrophoresis system; Invitrogen, Mountain View, CA) or 7.5% Tris acrylamide gels, as indicated in the figure legends, and analyzed by Western blotting (WesternBreeze immunodetection kit; Invitrogen) or silver staining (SilverQuest kit; Invitrogen),

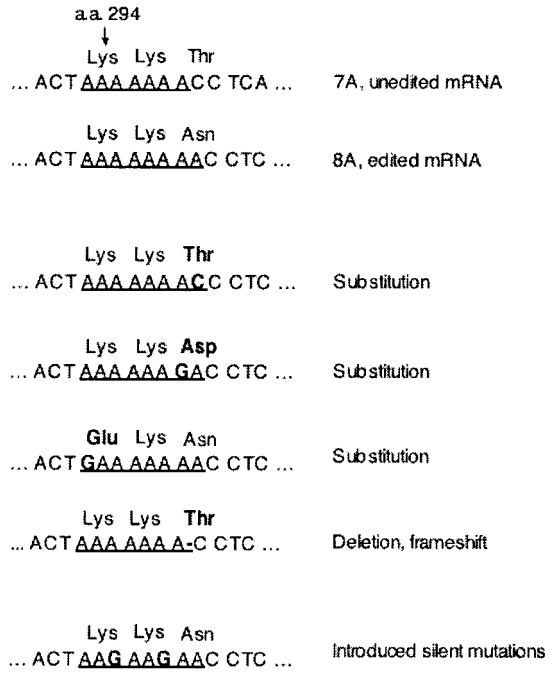

FIG. 2. Adventitious mutations detected in the editing site of the EV GP ORF in recovered HPIV3/EboGP and HPIV3/EboGP-NP viruses. The top line shows the positive-sense sequence of part of the editing site in the unedited version of EV GP mRNA, with encoded amino acids (a.a.) and their sequence positions in GP indicated and the homo-oligomeric A tract underlined. The next line shows the edited version of the mRNA containing a tract of eight A residues; this is the version that initially was inserted into the HPIV3 vector but proved to be unstable. The next four lines illustrate sequences from recovered viruses containing a nucleotide substitution or a nucleotide deletion that disrupts this run of eight A residues. The sequence at the bottom is an engineered mutant version of the edited mRNA that contains two A→G substitutions that interrupt the run of eight A residues without affecting amino acid coding; this version was used to make the second set of HPIV3/EboGP and HPIV3/EboGP-NP viruses that were used in this study.

all according to the manufacturer's recommendations. Magic XP marker proteins (Invitrogen) were electrophoresed in parallel as molecular weight markers. Densitometer scanning of the protein bands was performed using a Molecular Dynamics Personal Densitometer SI and the data analyzed using ImageQuant software (both from Molecular Dynamics, Sunnyvale, CA).

Virus neutralization titration. HPIV3 or HPIV3/EboGP was diluted in Opti-MEM medium (Invitrogen) containing 10% (vol/vol) of a commercial preparation of guinea pig complement (Cambrex Corporation, East Rutherford, New Jersey). Replicate aliquots, each containing $10^{5.2}$ PFU of virus, were mixed with an equal volume of a 1:10 or 1:40 dilution of a preparation of rabbit hyperimmune serum that had been raised against purified HPIV3 particles or against inactivated purified EV virions or were mixed with both sera. The mixtures were incubated for 1 h at 37°C and then subjected to plaque titration in LLC-MK2 and Vero cells to quantify residual infectious virus by counting the plaques following immunostaining. For that purpose, the cell monolayers were fixed in cold 80% methanol overnight, and the plaques were incubated sequentially with rabbit anti-HPIV3 antibodies (mentioned above) at 1:2,000, alkaline phosphatase-conjugated mouse anti-rabbit antibody at 1:2,000, and alkaline phosphatase substrate (both from Kirkegaard and Perry Laboratories, Gaithersburg, MD).

Guinea pig immunization. Three-month-old Hartley strain guinea pigs were obtained from Charles River Laboratories, Wilmington, MA, and were confirmed to be seronegative for HPIV3. Blood was collected, and the animals in groups of 9 or 10 were infected intranasally with $10^{5.3}$ PFU of recombinant viruses in 100 μl of Leibowitz L-15 medium (Invitrogen) (50 μl inhaled into each nostril). Twenty-eight days later, blood was collected and the animals were challenged with an intraperitoneal injection of 10^3 PFU of guinea pig-adapted

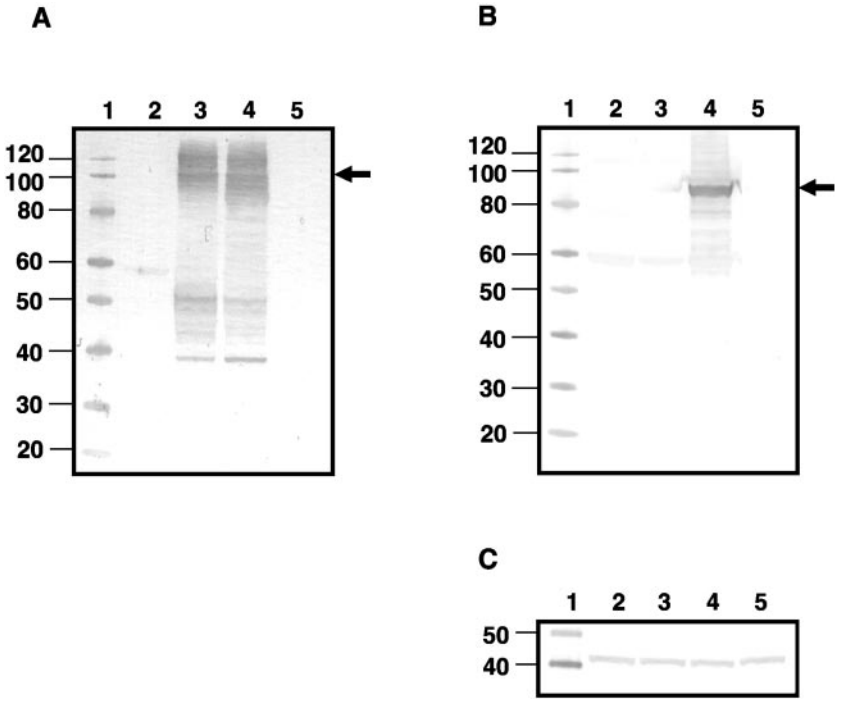

FIG. 3. Western blot analysis of cell-associated EV GP and NP expressed by the recombinant vectors. LLC-MK2 cells were infected with the recombinant viruses, and total cell lysates were prepared 24 h later, separated by electrophoresis on 4 to 12% bis-Tris acrylamide gradient gels under denaturing and reducing conditions, and subjected to Western blot analysis. Replicate blots were analyzed with rabbit anti-EV antibodies (A), guinea pig anti-NP antibodies (B), and a mouse monoclonal antibody against actin as a loading control (C). Lanes: 1, molecular weight markers; 2, HPIV3; 3, HPIV3/EboGP; 4, HPIV3/EboGP-NP; 5, mock infection. Molecular masses of the marker proteins (in kilodaltons) are shown in the left margins, and the positions of EV GP1 (A) and NP (B) are indicated with arrows.

EV diluted in sterile Hanks buffered salt solution. Seven days after the challenge, which is the peak time of the disease, blood was collected, four or five animals in each group were euthanatized, and the lungs, liver, and spleen were isolated for histologic analysis as described below. Among the remaining animals, those experiencing EV disease were sacrificed in extremis or collected shortly after death, and blood and tissues for histological analysis were collected. All remaining animals were sacrificed 22 days postchallenge, and blood and tissues for histological analysis were collected. During the immunization and challenge phases of the efficacy study, the animals were observed for signs of disease and weighed at 1- or 2-day intervals to assess their health. All procedures were performed in accordance with protocols and guidelines approved by the CDC Institutional Animal Care and Use Committee.

Quantitation of humoral responses. HPIV3-specific serum antibody titers in animals were determined using a hemagglutination inhibition (HAI) assay with guinea pig erythrocytes (49). EV-specific immunoglobulin G titers were determined using an enzyme-linked immunosorbent assay (ELISA) in which dilutions of animal sera were reacted with immobilized EV proteins. Specifically, a preparation of concentrated EV particles on dry ice was inactivated with 4 millirads of gamma irradiation by using a cobalt-60 high-energy gamma irradiator (MDS Nordion, Ottawa, Ontario, Canada) and purified by pelleting through a 20% (wt/vol) sucrose solution in Tris-buffered saline. The gamma irradiation step followed a CDC standard operating procedure that originally was qualified by titration on Vero cells. The preparation was treated with Tween 20 (Sigma, St. Louis, MO), diluted in phosphate-buffered saline, and used to coat 96-well, U-bottom polyvinyl chloride plates (Falcon 353911; Becton Dickinson, Franklin Lakes, NJ). Specific antibody binding was detected using a goat anti-guinea pig immunoglobulin G polyclonal serum conjugated with horseradish peroxidase and ABTS (2,2′-azinobis(3-ethylbenzthiazolinesulfonic acid) Peroxide Substrate System (KPL, Gaithersburg, MD). Absorbance at 405 nm was measured using a Tecan Spectrafluor fluorescence spectrophotometer (Tecan Trading AG, Switzerland).

Histological analysis. Tissue samples were processed for antigen detection by immunohistochemical (IHC) staining (56). Briefly, samples of spleen, liver, and lung tissues were fixed in buffered 10% formalin for 5 days. Tissues on wet ice were then exposed to gamma irradiation as described above to inactivate infectivity and processed for paraffin embedding, sectioning, and IHC staining. Specific EV antigen staining was accomplished by treating tissue sections with the following reagents in sequence: (i) an anti-EV serum that had been raised in rabbits by hyperimmunization with inactivated purified EV virions, (ii) biotinylated mouse anti-rabbit antibody, (iii) streptavidin-conjugated alkaline phosphatase, and (iv) naphthol fast red substrate (reagents ii to iv are components of the LSAB kit from Dako Corporation, Carpenteria, CA).

Electron microscopy. Virus particles from cultures of Vero E6 cells infected with recombinant HPIV3 or EV were used to generate negative-stained images. Formvar-carbon-coated nickel grids (300 mesh) were floated onto drops of tissue culture fluid for 10 min, and adsorbed particles were stained with 2% methylamine tungstate, pH 6.8 (Nanoprobes, Yaphank, NY). Stained viruses were visualized and images digitally recorded using a FEI Tecnai 12 BioTwin transmission electron microscope (FEI, Hillsboro, OR) operating at 100 to 120 kV.

RESULTS

Construction of HPIV3/EboGP and HPIV3/EboGP-NP. Reverse genetics was used to modify HPIV3 by inserting, between the P and M genes, a transcription cassette containing the EV GP ORF under the control of HPIV3 transcription signals, resulting in HPIV3/EboGP (Fig. 1). A second version was made to contain, in addition, a transcription cassette encoding EV NP inserted between the HN and L genes, resulting in HPIV3/EboGP-NP (Fig. 1). To confirm the sequences of the inserted genes, viral RNA was isolated and the genome regions containing the inserts were amplified by reverse transcription-PCR and sequenced. Surprisingly, we found mutations in the GP ORF editing site of every recovered virus. Specifically, three independently recovered preparations each of HPIV3/EboGP and HPIV3/EboGP-NP contained mutations in the

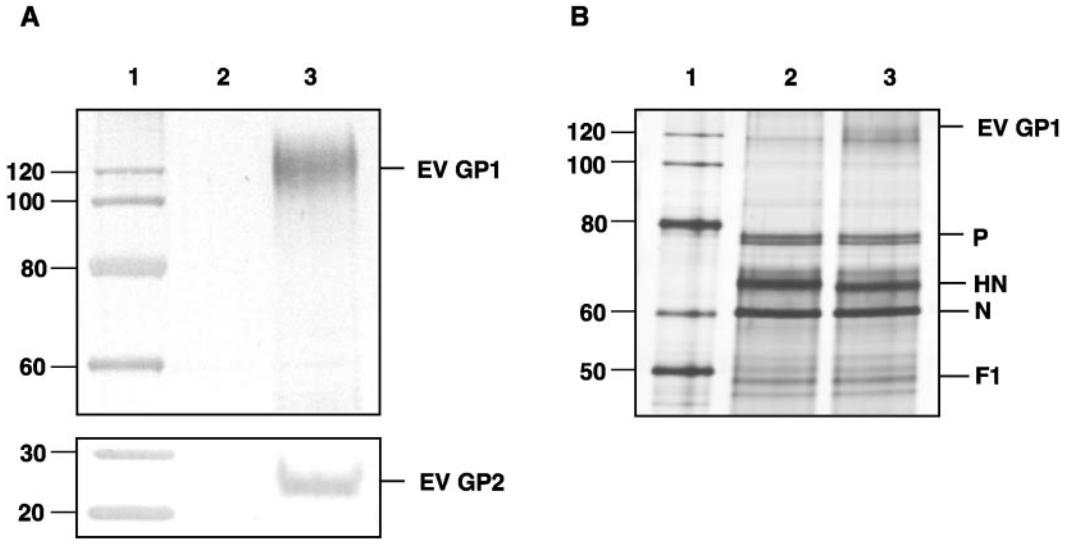

FIG. 4. Incorporation of EV GP1 and GP2 into recombinant virus particles. Purified HPIV3 and HPIV3/EboGP were prepared by sedimentation on discontinuous sucrose gradients, separated by electrophoresis on 4 to 12% (top panel A and panel B) or on 10% (bottom panel A) bis-Tris acrylamide gradient gels under denaturing and reducing conditions, and subjected to Western blot analysis with guinea pig anti-GP antibodies (top panel A) or rabbit hyperimmune serum that had been raised against inactivated purified EV virions (bottom panel A). A second gel containing the same array of samples was analyzed by silver straining (B). Lanes: 1, molecular weight markers; 2, HPIV3; 3, HPIV3/EboGP. Molecular masses of the marker proteins (in kilodaltons) are shown in the left margins, and positions of EV GP1, GP2, and the major HPIV3 proteins are shown in the right margins.

run of eight A residues that constitutes part of the editing site (Fig. 2). These mutations involved either a single nucleotide substitution that, in each case, resulted in a change in amino acid coding or a deletion of a single nucleotide resulting in an unedited ORF encoding sGP (Fig. 2). This sequence instability probably is a result of aberrant replication of this homo-oligomeric sequence by the HPIV3 polymerase; notably, homopolymer tracts larger than seven nucleotides do not otherwise occur in the HPIV3 genome. Mutations were not found elsewhere in the EV GP gene insert or in the EV NP gene insert of any recovered virus.

Since the changes in amino acid coding might adversely affect the immunogenicity of the encoded GP, we made a second set of HPIV3/EboGP and HPIV3/EboGP-NP viruses by using a version of the GP cDNA in which the run of eight A residues was modified by introducing two silent A→G substitutions (Fig. 2). Sequence analysis of this set of recovered viruses showed the GP or NP gene inserts to be free of mutations.

Expression of cell-associated EV GP and NP and incorporation of GP into the virus particles. LLC-MK2 cells were infected with the recombinant viruses and harvested 24 h later for Western blot analysis to examine the expression of cell-associated EV GP and NP (Fig. 3). EV GP was identified in cells infected with HPIV3/EboGP and HPIV3/EboGP-NP as a broad, disperse band with an electrophoretic mobility of approximately 100 to 160 kDa (Fig. 3A). This size range would encompass the previously described cell-associated forms of GP: the 110-kDa endoplasmic reticulum-specific form, the 160-kDa Golgi-specific form, and the 140-kDa GP1 subunit (52). In cells infected with HPIV3/EboGP-NP, a protein of approximately 90 kDa that corresponds to EV NP was identified (Fig. 3B). The vector-expressed GP1 and NP proteins comigrated with their counterparts from EV virus particles (see Fig. 9).

Several instances have been reported where foreign viral transmembrane proteins were incorporated into the envelopes of negative-strand viral vectors (36). To investigate whether GP was incorporated into the virion of the HPIV3 vector, we purified HPIV3 and HPIV3/EboGP virions by banding on discontinuous sucrose gradients and subjected them to Western blot analysis with antibodies against GP. As shown in Fig. 4A, GP1 and GP2 were detected in the preparation of HPIV3/EboGP and were absent, as expected, from the HPIV3 preparation. To evaluate the abundance of EV GP1 in the viral preparations, we subjected them to electrophoresis on a second gel that was analyzed by silver staining (Fig. 4B). Although the EV GP1 was not as abundant as the major HPIV3 structural proteins phosphoprotein (P), hemagglutinin-neuraminidase (HN) and N, and F1, it was clearly seen as an additional band. Densitometric analysis of the gel indicated that the EV GP band was approximately 13% as abundant as the HPIV3 HN protein. In addition, this comparison indicates that the presence of EV GP in the vector particle did not have any apparent effect on the content of the HPIV3 proteins, which was confirmed by densitometer analysis (not shown).

We also compared HPIV3, HPIV3/EboGP, HPIV3/EboGP-NP, and EV by electron microscopy using negative staining (Fig. 5). This showed that the virion morphologies of HPIV3/EboGP (Fig. 5B) and HPIV3/EboGP-NP (Fig. 5C) were essentially indistinguishable from that of HPIV3 (Fig. 5A) but were distinct from that of EV (Fig. 5D).

Expression of EV GP alters the CPE of the HPIV3 vector in cell culture. Since the expression of EV GP is known to cause increased CPE in cell culture (46), we examined whether expression of GP by HPIV3 was associated with a change in viral

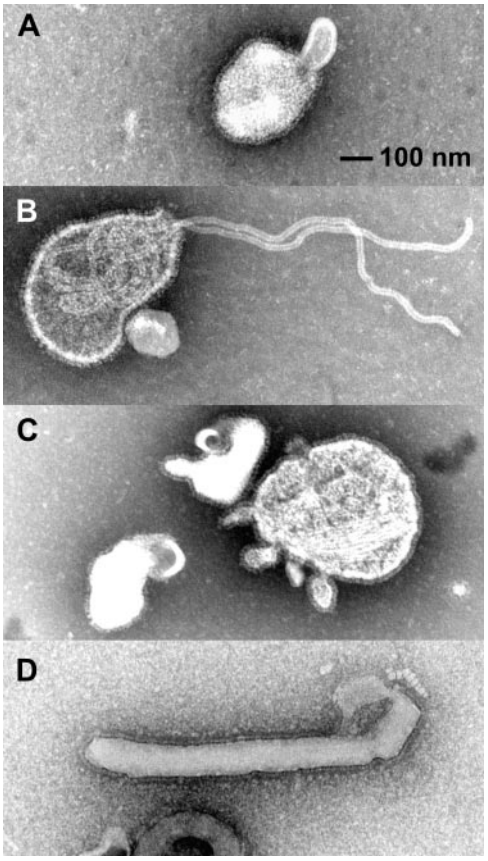

FIG. 5. Electron microscopy of virus particles. Shown are negative-stained images of HPIV3 (A), HPIV3/Ebo-GP (B), HPIV3/EboGP-NP (C), and EV (D). Glycoprotein peplomers are seen as a fringe along the outer edge of all virus particles, and extruding nucleocapsid is evident in panel B. Representative images are shown; in general, consistent differences between HPIV3 and its derivatives with EV gene inserts were not evident.

CPE. This was investigated in both LLC-MK2 cells, which are widely used for propagation of HPIV3, and Vero cells, which effectively support replication of EV. The cultures of LLC-MK2 and Vero cells were infected with the recombinant viruses. In LLC-MK2 cells infected with HPIV3, extensive syncytium formation with some cell rounding was observed by day 2 to 3, while infection with HPIV3/EboGP or HPIV3/EboGP-NP produced a massive cell rounding and detachment with little or no syncytium formation (Fig. 6) (infection with HPIV3/EboGP-NP is not shown since it was indistinguishable from that with HPIV3/EboGP). In Vero cells infected with HPIV3, little CPE was observed until 5 to 6 days after infection, when some cell rounding started to appear (not shown). However, in cells infected with HPIV3/EboGP or HPIV3/EboGP-NP, significant cell rounding was observed starting on day 2 (not shown), and by day 3, 50% to 70% of the cell monolayer consisted of round cells (Fig. 6). These studies demonstrated that insertion of a EV GP gene into the HPIV3 genome results in altered CPE characterized by cell rounding and detachment, consistent with previously published observations (55).

Anti-HPIV3 antibodies inhibit growth of HPIV3/EboGP but are incompletely neutralizing. The incorporation of EV GP into the virus particle had the potential to alter the neutralization and infectivity characteristics of the HPIV3 vector. To examine this question, $10^{5.2}$ PFU of HPIV3 or HPIV3/EboGP was mixed with an HPIV3-neutralizing antiserum, an EV-neutralizing antiserum, a mixture of both sera at dilutions of 1:10 and 1:40, or diluent (no antibody) in the presence of guinea pig complement and incubated for 1 h at 37°C, and the residual infectious virus was quantified by plaque titration in LLC-MK2 cells and Vero cells (Table 1). The monolayers were observed daily, and on day 7 the plaques were immunostained and counted. Incubation of HPIV3 with the HPIV3-specific antibodies resulted in a complete neutralization of infectivity, and plaque formation was observed in the samples without the antibodies. For HPIV3/EboGP, a reduced number of plaques appeared in all of the samples that had received the HPIV3-specific antibodies, indicating that HPIV3/EboGP, in contrast to HPIV3, was only partially neutralized by the HPIV3-specific antibodies. Incubation of HPIV3 with EV-specific antibodies did not result in a significant reduction of infectivity, whereas for HPIV3/EboGP, a strong reduction or a complete loss of infectivity was observed at the higher antibody concentration. Incubation of HPIV3/EboGP with mixture of the two antibodies resulted in loss of infectivity similar to that achieved with the EV antibodies alone. Thus, HPIV3-specific antibodies retarded, but did not completely inhibit, the spread of HPIV3/EboGP in cell culture, while EV-specific antibodies demonstrated a high level of neutralization of the virus.

HPIV3/EboGP and HPIV3/EboGP-NP are attenuated in cell culture. We compared the multistep growth kinetics of the recombinant viruses in LLC-MK2 cells and Vero cells (Fig. 7). The growth kinetics of HPIV3/EboGP and HPIV3/EboGP-NP were reduced compared to those of the parental virus, HPIV3, an effect that was more pronounced in LLC-MK2 cells than in Vero cells and was more pronounced with HPIV3/EboGP-NP than with HPIV3/EboGP. This is consistent with our previous findings that the insertion of additional transcriptional units into the HPIV3 genome results in reduced replication in cell culture and that this effect is increased with increasing length and number of inserts (43, 44). It also is possible that expression of GP contributed an attenuating effect, as was observed with a recombinant EV that was engineered to express an increased level of GP (53).

A single intranasal inoculation of guinea pigs with HPIV3/EboGP or HPIV3/EboGP-NP does not cause disease and induces a high-level EV-specific antibody immune response. The guinea pig model was selected to evaluate the safety, immunogenicity, and protective efficacy of the recombinant viruses. Guinea pigs are highly permissive to infection by and replication of HPIV3, although they do not exhibit overt HPIV3 disease. This experimental animal also is permissive to infection by and replication of a guinea pig-adapted strain of EV, and the infection results in extensive weight loss followed by death in essentially all animals (12, 51). Two-month-old guinea pigs seronegative for HPIV3 were immunized by a single intranasal inoculation of $10^{5.3}$ PFU of HPIV3, HPIV3/EboGP, or HPIV3/EboGP-NP, using 9 or 10 animals per group (Table 2). All of the animals appeared to be completely healthy, and all groups exhibited a steady increase in weight (Fig. 8A). On day 28 following immunization, high titers of antibody to the HPIV3 vector were detected in the blood of all three groups

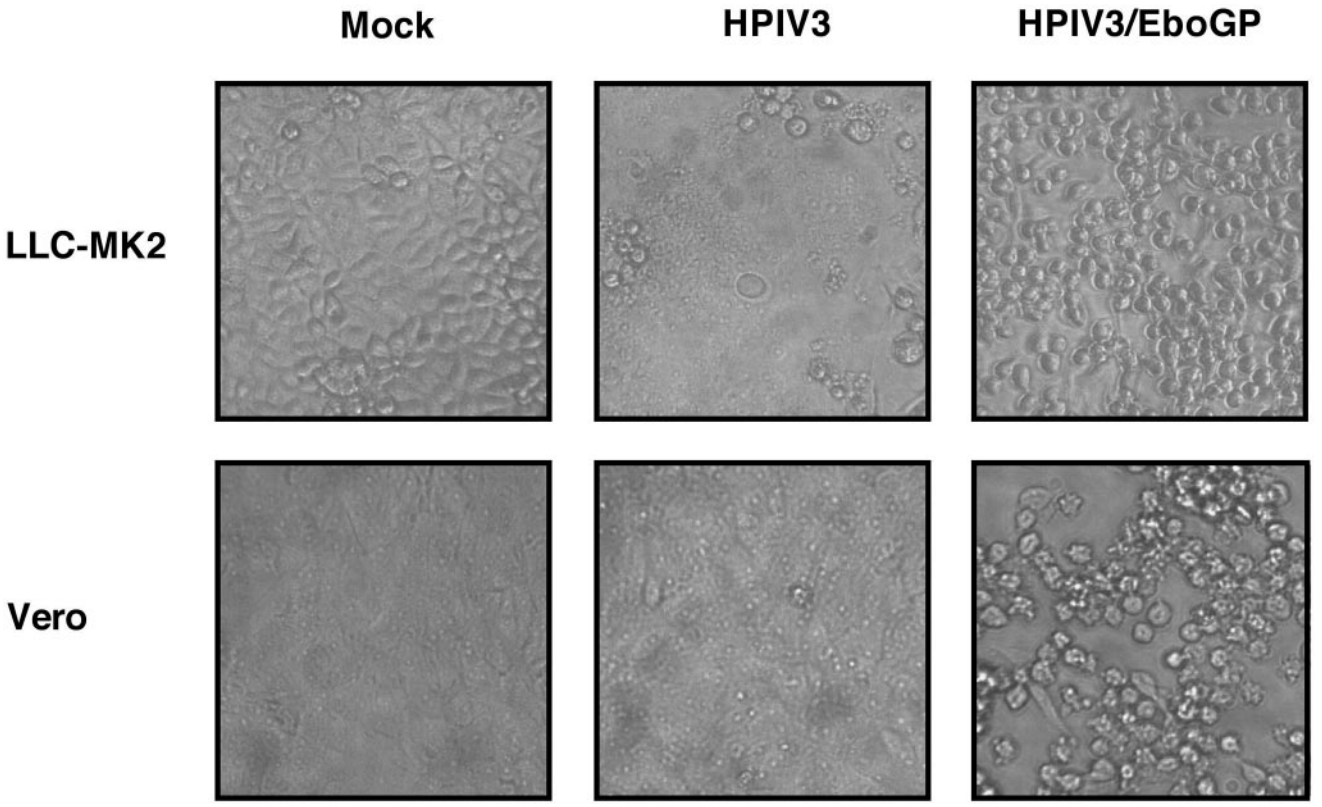

FIG. 6. CPE produced by the indicated recombinant viruses on day 3 after infection in LLC-MK2 and Vero cell cultures. Infections were performed at an input MOI of 0.2 PFU per cell. Infection with HPIV3/EboGP-NP produced CPE indistinguishable from that with HPIV3/EboGP and therefore is not shown.

(Table 2). On this admittedly indirect basis, the three immunizing viruses seemed to have replicated to comparable levels. Animals immunized with either of the two HPIV3/Ebo viruses, but not HPIV3, developed high titers of EV-specific serum antibodies measured by ELISA (Table 2).

Since the EV antigen used to detect an EV-specific response consisted of EV particles capable of detecting an antibody response to GP and other virion proteins, the specificity of the response to initial immunization was further characterized to confirm that HPIV3-vectored GP and NP EV antigens were

TABLE 1. Neutralization of HPIV3 and HPIV3/EboGP with anti-HPIV3 and/or anti-EV antibodies

Virus	Cells	Antibody dilution	Amt of infectious virus (log_{10} PFU) following neutralization with[a]:		
			Anti-HPIV3	Anti-EV	Anti-HPIV3 + anti-EV
HPIV3	LLC-MK2	1:10	<1.2	3.9	<1.2
		1:40	<1.2	ND[b]	<1.2
		No antibody	4.7	4.6	4.6
	Vero	1:10	<1.2	3.9	<1.2
		1:40	<1.2	ND	<1.2
		No antibody	4.8	4.8	4.7
HPIV3/EboGP	LLC-MK2	1:10	3.2	<1.2	1.2
		1:40	3.7	2.1	2.6
		No antibody	4.7	4.7	4.7
	Vero	1:10	3.6	1.7	1.9
		1:40	3.9	2.3	2.7
		No antibody	4.9	5.1	5.2

[a] The indicated viruses ($10^{5.2}$ PFU) were incubated with the indicated dilution of anti-HPIV3 antibodies, anti-EV antibodies, or their mixture in the presence of complement. After the incubation, the residual infectivity was determined on day 7 by plaque titration in the indicated cell lines.
[b] ND, not determined.

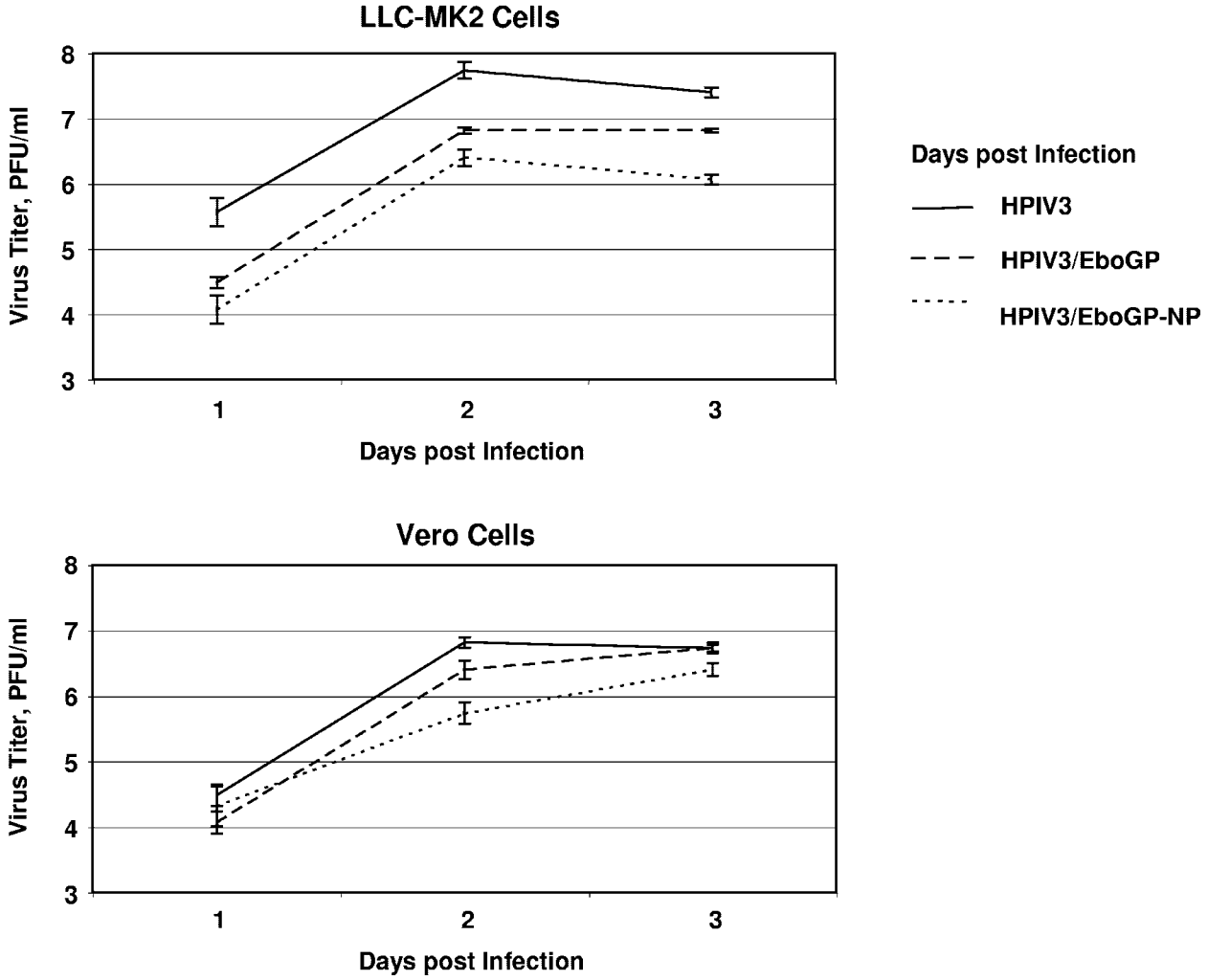

FIG. 7. Multistep growth kinetics of the indicated recombinant viruses in LLC-MK2 and Vero cells. Cell monolayers were infected with the indicated viruses at an input MOI of 0.001 PFU per cell. Supernatants were harvested at 24-h intervals and flash frozen, and virus titers were determined in LLC-MK2 cells and expressed as PFU per milliliter. Mean values and standard error from triplicate samples are shown. These data are from a representative experiment out of a total of two independent experiments.

immunogenic. This was done by Western blot analysis using the purified HPIV3/Ebo viruses or EV as sources of antigen (Fig. 9). An anti-GP response from an animal immunized with HPIV3/EboGP-NP (Fig. 9C) was detected with EV GP antigen using concentrated HPIV3/EboGP (lane 3), HPIV3/EboGP-NP (lane 4), and EV (lane 5). An anti-NP response (Fig. 9C) was detected with EV NP antigen from concentrated EV (lane 5) but not HPIV3/EboGP-NP (lane 4), since EV NP is not present in the viral particles of the construct. Serum from a control animal immunized with HPIV3 reacted with neither of the two EV antigens (Fig. 9B).

The immunization is highly protective against EV challenge. At 28 days following immunization, all of the animals were challenged intraperitoneally with 10^3 PFU of guinea pig-adapted EV, a dose that is highly lethal. All of the animals that had been immunized with the HPIV3 control virus developed an EV infection that was accompanied by weight loss (Fig. 8B). These animals demonstrated high-level viremia and high levels of EV antigen in blood (Table 2); in spleen, liver, and lungs (Fig. 10); and, in one case, in gallbladder. All of the animals in this group died 8 to 10 days after the challenge. In the groups that had been immunized with HPIV3/EboGP or HPIV3/EboGP-NP, there was no significant weight loss (Fig. 8B) or signs of illness, and EV or EV antigen was not detected in the blood on day 7 or 22 after the challenge (Table 2) or in lung, liver, and spleen tissue harvested on day 7 (Fig. 10) or 22 (data not shown). All of the animals were alive and healthy when sacrificed at 7 or 22 days postinfection (Table 2; Fig. 8B).

Animals that had been immunized with HPIV3/EboGP or HPIV3/EboGP-NP had some increases in EV-specific serum antibodies on day 22 postchallenge (Table 2). The possible explanations of this phenomenon are the following: (i) a continued rise in the titer due to immunization; (ii) a boosting effect of the EV antigen present in the challenge virus; (iii) limited, undetected, asymptomatic replication of EV after the challenge; or (iv) a combination of these factors.

DISCUSSION

This is the first study demonstrating that intranasal immunization with a live respiratory virus vector expressing a pro-

TABLE 2. Immunogenicity and protective efficacy of HPIV3/EboGP and HPIV3/EboGP-NP in guinea pigs

Immunizing virus (no. of animals)	Response to immunization (reciprocal $\log_2 \pm$ SE)[a]				Response to challenge with EV (mean $\pm$ SE)[b]				
	Antibodies to HPIV3 (HAI)		Antibodies to EV (ELISA)		EV antigen in blood (ELISA, reciprocal $\log_2$), day 7	EV titer in blood, (PFU/ml, reciprocal $\log_{10}$), day 7	Mortality, %	Antibodies to EV (ELISA, reciprocal $\log_2$)	
	Day 0	Day 28	Day 0	Day 28				Day 7	Day 22
HPIV3 (9)	<2.0	7.7 ± 0.2	<7.6	<7.6	13.9 ± 0.3	6.7 ± 0.2[c]	100	<7.6[d]	ND[e]
HPIV3/EboGP (10)	<2.0	6.6 ± 0.1	<7.6	13.6 ± 0.0	<4.3	<1.0	0	14.2 ± 0.3	16.0 ± 0.3
HPIV3/EboGP-NP (9)	<2.0	7.3 ± 0.2	<7.6	13.9 ± 0.2	<4.3	<1.0	0	14.1 ± 0.3	17.2 ± 0.3

[a] Animals were immunized on day 0 with a single intranasal inoculation of $10^{5.3}$ PFU of the indicated virus. Reciprocal $\log_2$ of serum endpoint dilutions are indicated.
[b] Animals were challenged on day 28 (day 0 of the challenge) with 10^3 PFU of EV administered intraperitoneally.
[c] For the animals that had EV titers in blood exceeding 7.2×10^7 PFU/ml, that value was assigned for calculation of the mean.
[d] Antibody levels were below the detection limit in all animals except for a single animal (animal 7), in which a titer of EV-specific antibodies at the level of 1:1,280 was detected.
[e] ND, not determined. The animals in this group developed EV infection and died on days 8 to 10 postchallenge.

tective antigen of an agent of severe viral hemorrhagic fever can induce a systemic protective immunity against a lethal dose of that agent. Remarkably, there was no evidence of EV infection in animals previously immunized with HPIV3/EboGP or HPIV3/EboGP-NP. The lack of EV in the blood and the target organs (liver, spleen, and lungs) of HPIV3/Ebo-immunized animals indicates that a high level of protection was achieved, although there may have been a low level of challenge virus replication that was below the level of detection of our assays. However, evaluation of the constructs in nonhuman

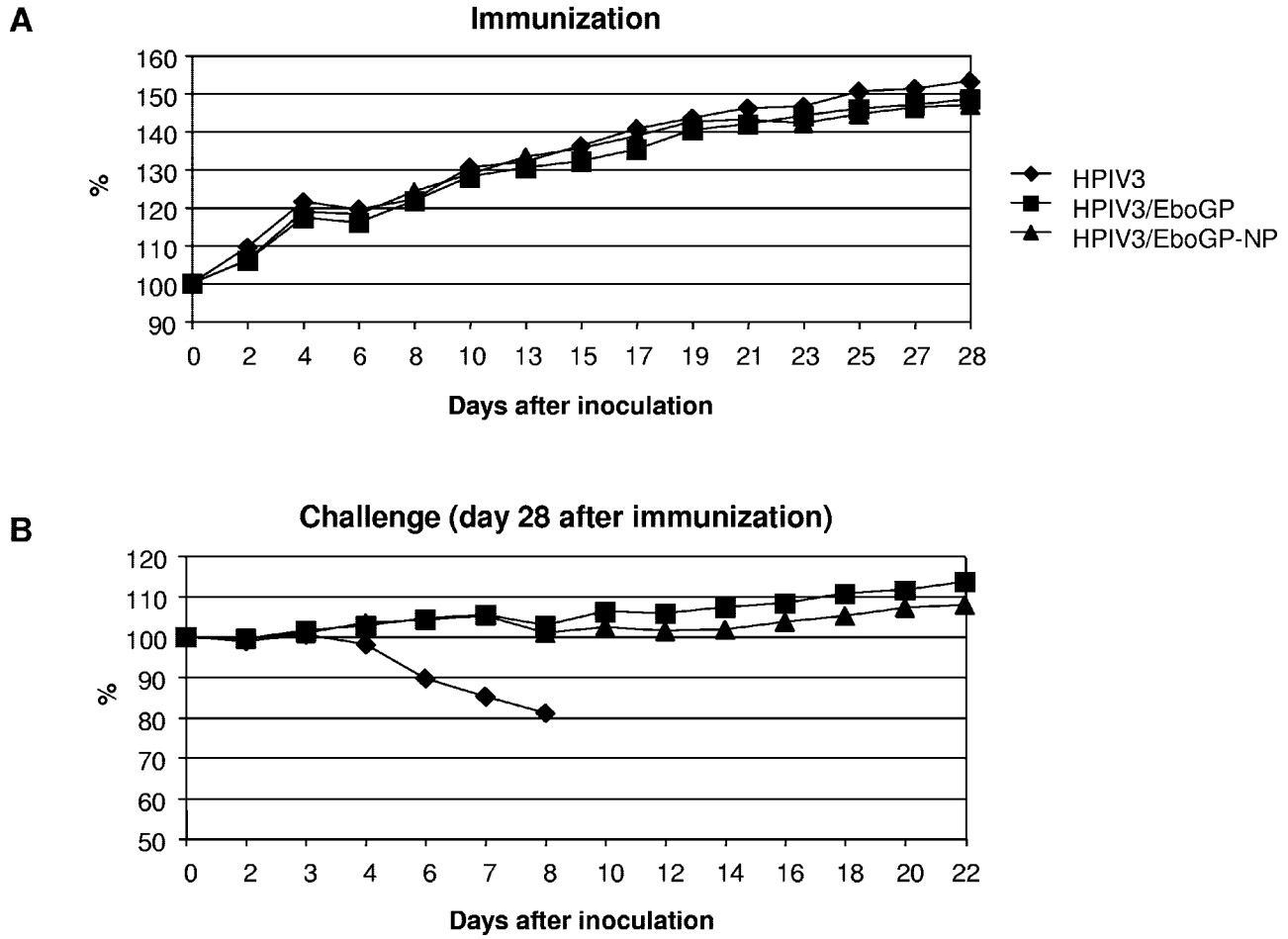

FIG. 8. Mean body weights of the guinea pigs in the experimental groups that received the indicated recombinant viruses following the initial immunizing infection (A) and following the EV challenge on day 28 (B). The mean weights are plotted as percentages relative to the mean weights on the day of immunization (A) or challenge (B). Of the five animals in the control (HPIV3-vaccinated) group that were not sacrificed on day 7 postchallenge, two animals died on day 8, one animal on day 9, and two animals on day 10.

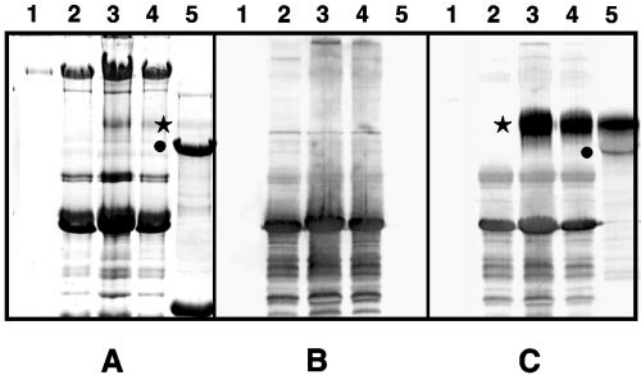

FIG. 9. Specificity of guinea pig serum antibodies following the initial immunization. The following samples were separated in three replicate 7.5% SDS-polyacrylamide gels: mock-purified virus from uninfected cells (lane 1), purified HPIV3 (lane 2), purified HPIV3/EboGP (lane 3), purified HPIV3/GP-NP (lane 4), and purified EV (lane 5). One replicate gel was stained with Coomassie blue (A), and the other two were subjected to Western blot analysis with antiserum from a representative individual guinea pig taken on day 28 after immunization with HPIV3 (B) or HPIV3/EboGP-NP (C). The positions of EV GP1 and NP are shown by stars and circles, respectively, in panels A and C. The poor detection of GP1 in lane 5 of panel A probably reflects inefficient reactivity of the glycoprotein with the Coomassie stain due to the high density of the carbohydrate side chains. The lack of NP in lane 4 of panel C indicates that EV NP is not incorporated into the HPIV3 vector particles.

primates will be necessary, since protective immunity induced in rodent models does not guarantee a similar outcome when tested in monkeys (21, 35). It is noteworthy that the expression of EV GP and NP by HPIV3 was not associated with disease in an animal model that is permissive to replication by both viruses and is very sensitive to EV disease. While it will be important to examine infection by HPIV3/EboGP and HPIV3/EboGP-NP more fully, including monitoring virus titers and tissue distribution, the available evidence indicates that expression of these EV proteins in vivo did not confer EV-specific pathogenicity to the HPIV3 vector. We believe that the present study would have provided for sensitive detection of any EV-specific pathogenicity conferred to the HPIV3 vector, because the 50% lethal dose of this strain of EV in guinea pigs was approximately 0.0025 PFU (see Materials and Methods) and the HPIV3-based vectors were administered at the much higher dose of 5.3 $\log_{10}$ PFU.

This study shows that the EV GP protein is necessary and sufficient for induction of protective immunity against the virus, which is consistent with previously published data with the guinea pig model (34, 54) and the primate model (24, 47). The second EV protein, NP, was previously shown to induce a short-term protective response in guinea pigs (54) and contributed to a protective immune response in primates through the induction of cytotoxic T lymphocytes (45). However, in our study the possible contribution of NP in HPIV3/EboGP-NP to the induction of a protective immunity was obscured by the high level of protection induced by the GP protein. Therefore,

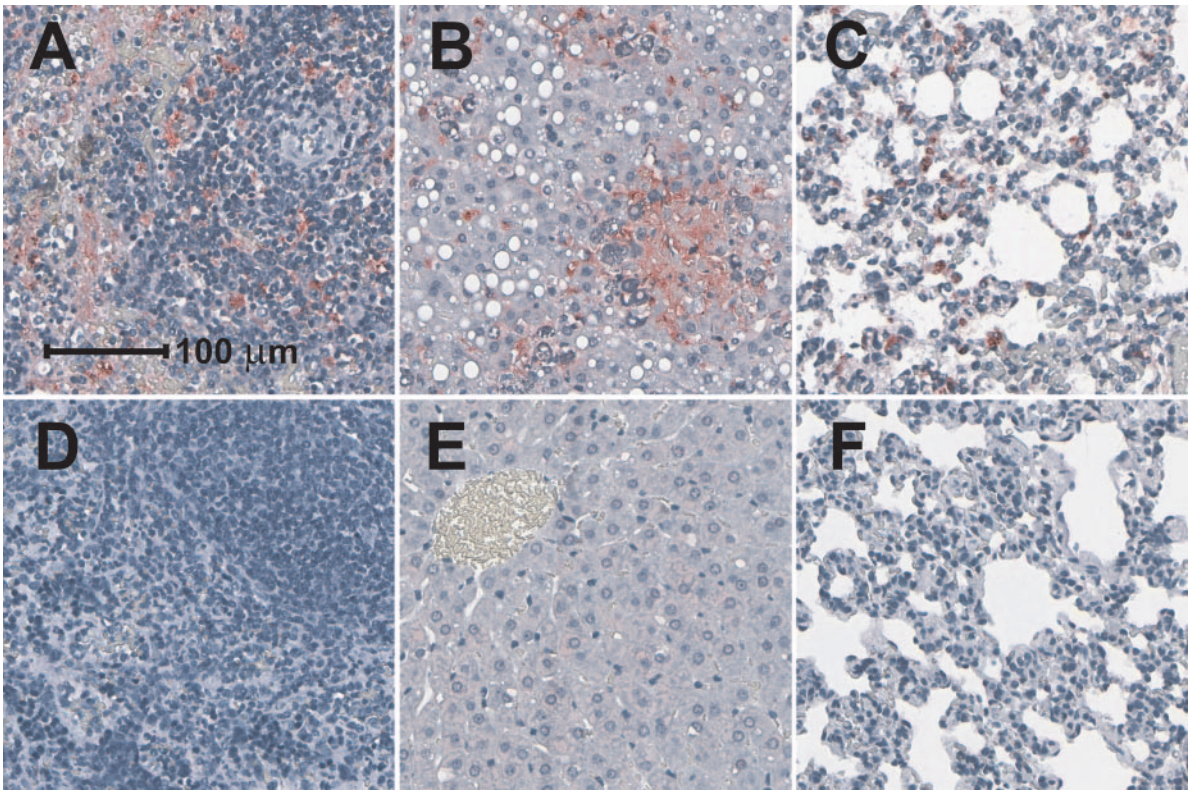

FIG. 10. EV antigen detection in internal organs of guinea pigs on day 7 after the challenge. Shown are representative examples of IHC staining of spleen (A and D), liver (B and E), and lung (C and F) tissues from a control animal immunized with HPIV3 (A, B and C) and from an animal immunized with HPIV3/EboGP-NP (D, E and F). Areas of the section containing EV antigen are stained red. Bar, 100 μm.

the relative contributions of the antibody response and cytotoxic T-cell response to the individual EV proteins after immunization with HPIV3/EboGP and HPIV3/EboGP-NP will be examined in a separate study.

Expression of GP in cell culture in the absence of the other EV proteins was previously shown to result in increased CPE (46). This also was observed in the present study for GP expressed from HPIV3. However, this was not associated with increased virulence in the guinea pig model, and this is not the first time that we have observed a lack of correlation between CPE in vitro and virulence in vivo. For example, repositioning of the fusion F glycoprotein of RSV to be promoter proximal increased its expression and CPE in vitro, but a change in virulence was not observed in mice (27). Also, when the expression of all RSV genes (including F) was increased through deletion of the M2-2 regulatory protein, a considerable increase in CPE was observed in vitro, but this recombinant RSV was highly attenuated in chimpanzees (4, 48). Human metapneumovirus in which the cleavage site of the F protein was modified to be trypsin independent (which for biosafety reasons was evaluated in an attenuated background) exhibited greater CPE in vitro with no change in virulence in hamsters (S. Biacchesi, B. R. Murphy, P. L. Collins, et al., unpublished data). It perhaps is not surprising that CPE in vitro does not necessarily predict virulence in vivo, since infected cells in vivo are killed in any event, either by viral factors such as syncytium formation, by apoptosis, or by host immunity. The increased CPE observed in vitro was accompanied by a decrease in replication of HPIV3/EboGP and HPIV3/EboGP-NP compared to that of HPIV3.

Expression of GP by HPIV3 resulted in a low level of incorporation of the foreign glycoprotein into the HPIV3 virus particle, whereas NP was not detected in HPIV3/EboGP-NP virions. Since EV GP mediates both attachment and penetration, it had the potential to initiate infection by the HPIV3 vector independently of the HN and F proteins of the vector, and thus it was possible that HPIV3 virion-associated GP might be able to mediate infection in the presence of neutralizing antibodies to HPIV3. Indeed, this seemed to occur: the HPIV3-neutralizing antibodies that completely neutralized the HPIV3 vector only weakly neutralized HPIV3/EboGP infectivity due to the presence of EV GP in the virions. Surprisingly, the EV antibodies were highly efficient in neutralizing the infectivity of HPIV3/EboGP. Thus, virions containing both HN and F glycoproteins of HPIV3 and GP of EV were more efficiently neutralized by EV antibodies than HPIV3 despite the greater amount of the HPIV3 glycoproteins than EV GP. The reason for this observation remains to be understood. In any event, the presence of HPIV3 and EV glycoproteins in the virions did not detectably alter the pathogenesis of HPIV3 in vivo. This was reassuring but not unexpected. The cellular receptor for HPIV3, sialic acid, is widely distributed, and thus HPIV3 infection and tissue tropism probably are not limited by receptor availability. In addition, HPIV3 can readily disseminate systemically from the lungs to other organs in experimental animals that have been immunosuppressed (15, 16). Thus, HPIV3 already has the capability to spread widely from the respiratory tract.

We chose HPIV3 as a model to evaluate the potential of respiratory viruses as a vector against EV because HPIV3 readily infects and induces immune responses in guinea pigs and rhesus monkeys, which are appropriate experimental animals for evaluating EV infection and disease. HPIV3 is a common cause of respiratory infections in infants and children, and a series of cDNA-derived HPIV3 mutants are being developed and evaluated as candidate pediatric vaccines against HPIV3 (30). Thus, an attenuated version of HPIV3 could be appropriate for use as a pediatric vaccine vector for EV and other pathogens. However, most of the adult human population is seropositive for HPIV3 due to natural exposure. The prevalence of immunity to the HPIV3 vector would restrict its replication (11), resulting in a reduced immune response to the expressed foreign antigen. This problem would occur for any vector that is based on a common human pathogen, such as adenovirus type 5 vector. On the other hand, reinfection with HPIV3 in adults is common (10), suggesting that at least a limited level of viral replication can occur in seropositive individuals. Moreover, incorporation of EV GP into HPIV3/EboGP virus particles and the infectivity of the virus in cell cultures in the presence of anti-HPIV3 antibodies suggest that HPIV3/EboGP may have some effectiveness in HPIV3-seropositive hosts. This issue will be explored in a separate study using HPIV3-seropositive guinea pigs. An alternative strategy is to develop vectors based on nonhuman paramyxoviruses that are antigenically unrelated to major human pathogens and for which the human adult population is seronegative, such as the avian Newcastle disease virus (31, 32). We recently showed that this virus is highly attenuated in nonhuman primates and induced a strong immune response against an expressed foreign antigen (8) and therefore represents a promising vaccine vector.

Paramyxovirus-vectored intranasal vaccines against hemorrhagic fever viruses such as EV and Marburg virus could prove useful to contain outbreaks of these diseases and to protect health care workers. This type of vaccine would have several important advantages. First, since aerosols of EV are known to be infectious (23, 42) and might be used in an act of bioterrorism, the systemic and mucosal immunity induced by an intranasal vaccination could provide rapid and effective protection against such public health threats. Second, intranasal immunization would not require highly trained medical personnel, and immunization of large numbers of individuals in outbreak settings could be more readily accomplished by this route than by parenteral immunization. Third, intranasal immunization precludes the spread of blood-borne pathogens, which can occur during parenteral immunization. Fourth, most of the paramyxoviruses can grow well in Vero suspension cell cultures, which would make their manufacturing economically feasible. This is in contrast to some other vector systems, such as those based on replication-deficient adenoviruses, which require costly helper cell lines and high-dose immunizations. In addition, intranasal immunization can be used to boost immune response after parenterally administered vaccine, such as that based on adenovirus or vesicular stomatitis virus (24, 45, 47). In any case, it would be valuable to have several platforms for vector-based vaccines in order to control outbreaks of various emerging pathogens, since development of an immune response against one particular vector would probably make it inefficient for subsequent vaccination of the same individual.

ACKNOWLEDGMENTS

We thank Elaine Lamirande for excellent technical assistance, Ernest Williams and Fatemeh Davoodi for performing HAI assays, Mario Skiadopoulos for providing rabbit anti-HPIV3 serum, Patricia Greer for processing tissues for IHC, and Charles Humphrey for producing the electron microscopy images.

This project was funded as a part of the NIAID Intramural Program.

REFERENCES

1. **Baize, S., E. M. Leroy, M. C. Georges-Courbot, M. Capron, J. Lansoud-Soukate, P. Debre, S. P. Fisher-Hoch, J. B. McCormick, and A. J. Georges.** 1999. Defective humoral responses and extensive intravascular apoptosis are associated with fatal outcome in Ebola virus-infected patients. Nat. Med. **5:**423–426.
2. **Baize, S., E. M. Leroy, E. Mavoungou, and S. P. Fisher-Hoch.** 2000. Apoptosis in fatal Ebola infection. Does the virus toll the bell for immune system? Apoptosis **5:**5–7.
3. **Basler, C. F., X. Wang, E. Muhlberger, V. Volchkov, J. Paragas, H. D. Klenk, A. Garcia-Sastre, and P. Palese.** 2000. The Ebola virus VP35 protein functions as a type I IFN antagonist. Proc. Natl. Acad. Sci. USA **97:**12289–12294.
4. **Bermingham, A., and P. L. Collins.** 1999. The M2-2 protein of human respiratory syncytial virus is a regulatory factor involved in the balance between RNA replication and transcription. Proc. Natl. Acad. Sci. USA **96:**11259–11264.
5. **Bosio, C. M., M. J. Aman, C. Grogan, R. Hogan, G. Ruthel, D. Negley, M. Mohamadzadeh, S. Bavari, and A. Schmaljohn.** 2003. Ebola and Marburg viruses replicate in monocyte-derived dendritic cells without inducing the production of cytokines and full maturation. J. Infect. Dis. **188:**1630–1638.
6. **Bray, M., and T. W. Geisbert.** 2005. Ebola virus: the role of macrophages and dendritic cells in the pathogenesis of Ebola hemorrhagic fever. Int. J. Biochem. Cell. Biol. **37:**1560–1566.
7. **Buchholz, U. J., S. Finke, and K. K. Conzelmann.** 1999. Generation of bovine respiratory syncytial virus (BRSV) from cDNA: BRSV NS2 is not essential for virus replication in tissue culture, and the human RSV leader region acts as a functional BRSV genome promoter. J. Virol. **73:**251–259.
8. **Bukreyev, A., Z. Huang, L. Yang, S. Elankumaran, M. St. Claire, B. R. Murphy, S. K. Samal, and P. L. Collins.** 2005. Recombinant Newcastle disease virus expressing a foreign viral antigen is attenuated and highly immunogenic in primates. J. Virol. **79:**13275–13284.
9. **Bukreyev, A., E. W. Lamirande, U. J. Buchholz, L. N. Vogel, W. R. Elkins, M. St Claire, B. R. Murphy, K. Subbarao, and P. L. Collins.** 2004. Mucosal immunisation of African green monkeys (Cercopithecus aethiops) with an attenuated parainfluenza virus expressing the SARS coronavirus spike protein for the prevention of SARS. Lancet **363:**2122–2127.
10. **Chanock, R. M., B. R. Murphy, and P. L. Collins.** 2001. Parainfluenza viruses, p. 1341–1379. *In* D. M. Knipe, P. M. Howley, D. E. Griffin, R. A. Lamb, M. A. Martin, B. Roizman, and S. E. Straus (ed.), Fields virology, 4th ed., vol. 1. Lippincott-Raven Publishers, Philadelphia, Pa.
11. **Clements, M. L., R. B. Belshe, J. King, F. Newman, T. U. Westblom, E. L. Tierney, W. T. London, and B. R. Murphy.** 1991. Evaluation of bovine, cold-adapted human, and wild-type human parainfluenza type 3 viruses in adult volunteers and in chimpanzees. J. Clin. Microbiol. **29:**1175–1182.
12. **Connolly, B. M., K. E. Steele, K. J. Davis, T. W. Geisbert, W. M. Kell, N. K. Jaax, and P. B. Jahrling.** 1999. Pathogenesis of experimental Ebola virus infection in guinea pigs. J. Infect. Dis. **179**(Suppl. 1)**:**S203–S217.
13. **Durbin, A., S. Hall, J. Siew, S. Whitehead, P. Collins, and B. Murphy.** 1997. Recovery of infectious human parainfluenza virus type 3 from cDNA. Virology **235:**232.
14. **Feldmann, H., S. Jones, H. D. Klenk, and H. J. Schnittler.** 2003. Ebola virus: from discovery to vaccine. Nat. Rev. Immunol. **3:**677–685.
15. **Fishaut, M., D. Tubergen, and K. McIntosh.** 1980. Cellular response to respiratory viruses with particular reference to children with disorders of cell-mediated immunity. J. Pediatr. **96:**179–186.
16. **Frank, J. A., Jr., R. W. Warren, J. A. Tucker, J. Zeller, and C. M. Wilfert.** 1983. Disseminated parainfluenza infection in a child with severe combined immunodeficiency. Am. J. Dis. Child. **137:**1172–1174.
17. **Geisbert, T. W., L. E. Hensley, T. R. Gibb, K. E. Steele, N. K. Jaax, and P. B. Jahrling.** 2000. Apoptosis induced in vitro and in vivo during infection by Ebola and Marburg viruses. Lab. Investig. **80:**171–186.
18. **Geisbert, T. W., L. E. Hensley, T. Larsen, H. A. Young, D. S. Reed, J. B. Geisbert, D. P. Scott, E. Kagan, P. B. Jahrling, and K. J. Davis.** 2003. Pathogenesis of Ebola hemorrhagic fever in cynomolgus macaques: evidence that dendritic cells are early and sustained targets of infection. Am. J. Pathol. **163:**2347–2370.
19. **Geisbert, T. W., and P. B. Jahrling.** 2004. Exotic emerging viral diseases: progress and challenges. Nat. Med. **10:**S110–S121.
20. **Geisbert, T. W., and P. B. Jahrling.** 2003. Towards a vaccine against Ebola virus. Expert Rev. Vaccines **2:**777–789.
21. **Geisbert, T. W., P. Pushko, K. Anderson, J. Smith, K. J. Davis, and P. B. Jahrling.** 2002. Evaluation in nonhuman primates of vaccines against Ebola virus. Emerg. Infect. Dis. **8:**503–507.
22. **Geisbert, T. W., H. A. Young, P. B. Jahrling, K. J. Davis, T. Larsen, E. Kagan, and L. E. Hensley.** 2003. Pathogenesis of Ebola hemorrhagic fever in primate models: evidence that hemorrhage is not a direct effect of virus-induced cytolysis of endothelial cells. Am. J. Pathol. **163:**2371–2382.
23. **Johnson, E., N. Jaax, J. White, and P. Jahrling.** 1995. Lethal experimental infections of rhesus monkeys by aerosolized Ebola virus. Int. J. Exp. Pathol. **76:**227–236.
24. **Jones, S. M., H. Feldmann, U. Stroher, J. B. Geisbert, L. Fernando, A. Grolla, H. D. Klenk, N. J. Sullivan, V. E. Volchkov, E. A. Fritz, K. M. Daddario, L. E. Hensley, P. B. Jahrling, and T. W. Geisbert.** 2005. Live attenuated recombinant vaccine protects nonhuman primates against Ebola and Marburg viruses. Nat. Med. **11:**786–790.
25. **Kemble, G., and H. Greenberg.** 2003. Novel generations of influenza vaccines. Vaccine **21:**1789–1795.
26. **Kolakofsky, D., T. Pelet, D. Garcin, S. Hausmann, J. Curran, and L. Roux.** 1998. Paramyxovirus RNA synthesis and the requirement for hexamer genome length: the rule of six revisited. J. Virol. **72:**891–899.
27. **Krempl, C., B. R. Murphy, and P. L. Collins.** 2002. Recombinant respiratory syncytial virus with the G and F genes shifted to the promoter-proximal positions. J. Virol. **76:**11931–11942.
28. **Mahanty, S., and M. Bray.** 2004. Pathogenesis of filoviral haemorrhagic fevers. Lancet Infect. Dis. **4:**487–498.
29. **Mahanty, S., K. Hutchinson, S. Agarwal, M. McRae, P. E. Rollin, and B. Pulendran.** 2003. Cutting edge: impairment of dendritic cells and adaptive immunity by Ebola and Lassa viruses. J. Immunol. **170:**2797–2801.
30. **Murphy, B. R., and P. L. Collins.** 2002. Live-attenuated virus vaccines for respiratory syncytial and parainfluenza viruses: applications of reverse genetics. J. Clin. Investig. **110:**21–27.
31. **Nakaya, T., J. Cros, M. S. Park, Y. Nakaya, H. Zheng, A. Sagrera, E. Villar, A. Garcia-Sastre, and P. Palese.** 2001. Recombinant Newcastle disease virus as a vaccine vector. J. Virol. **75:**11868–11873.
32. **Nakaya, Y., T. Nakaya, M. S. Park, J. Cros, J. Imanishi, P. Palese, and A. Garcia-Sastre.** 2004. Induction of cellular immune responses to simian immunodeficiency virus Gag by two recombinant negative-strand RNA virus vectors. J. Virol. **78:**9366–9375.
33. **Pourrut, X., B. Kumulungui, T. Wittmann, G. Moussavou, A. Delicat, P. Yaba, D. Nkoghe, J. P. Gonzalez, and E. M. Leroy.** 2005. The natural history of Ebola virus in Africa. Microbes Infect. **7:**1005–1014.
34. **Pushko, P., M. Bray, G. V. Ludwig, M. Parker, A. Schmaljohn, A. Sanchez, P. B. Jahrling, and J. F. Smith.** 2000. Recombinant RNA replicons derived from attenuated Venezuelan equine encephalitis virus protect guinea pigs and mice from Ebola hemorrhagic fever virus. Vaccine **19:**142–153.
35. **Pushko, P., J. Geisbert, M. Parker, P. Jahrling, and J. Smith.** 2001. Individual and bivalent vaccines based on alphavirus replicons protect guinea pigs against infection with Lassa and Ebola viruses. J. Virol. **75:**11677–11685.
36. **Roberts, A., L. Buonocore, R. Price, J. Forman, and J. K. Rose.** 1999. Attenuated vesicular stomatitis viruses as vaccine vectors. J. Virol. **73:**3723–3732.
37. **Rouquet, P., J. M. Froment, M. Bermejo, P. Yaba, A. Delicat, P. E. Rollin, and E. M. Leroy.** 2005. Wild animal mortality monitoring and human Ebola outbreaks, Gabon and Republic of Congo, 2001–2003. Emerg. Infect. Dis. **11:**283–290.
38. **Sanchez, A., A. S. Khan, S. R. Zaki, G. J. Nabel, T. G. Ksiazek, and C. J. Peters.** 2001. Filoviridae: Marburg and Ebola viruses, p. 1279–1304. *In* D. M. Knipe, P. M. Howley, D. E. Griffin, R. A. Lamb, M. A. Martin, B. Roizman, and S. E. Straus (ed.), Fields virology, 4th ed., vol. 1. Lippincott-Raven Publishers, Philadelphia, Pa.
39. **Sanchez, A., and M. P. Kiley.** 1987. Identification and analysis of Ebola virus messenger RNA. Virology **157:**414–420.
40. **Sanchez, A., M. P. Kiley, B. P. Holloway, and D. D. Auperin.** 1993. Sequence analysis of the Ebola virus genome: organization, genetic elements, and comparison with the genome of Marburg virus. Virus Res. **29:**215–240.
41. **Sanchez, A., S. G. Trappier, B. W. Mahy, C. J. Peters, and S. T. Nichol.** 1996. The virion glycoproteins of Ebola viruses are encoded in two reading frames and are expressed through transcriptional editing. Proc. Natl. Acad. Sci. USA **93:**3602–3607.
42. **Sergeev, A. N., M. Lub, G. P'Iankova, O., and L. A. Kotliarov.** 1995. The efficacy of the emergency prophylactic and therapeutic actions of immunomodulators in experimental filovirus infections. Antibiot. Khimioter. **40:**24–27.
43. **Skiadopoulos, M. H., S. R. Surman, A. P. Durbin, P. L. Collins, and B. R. Murphy.** 2000. Long nucleotide insertions between the HN and L protein coding regions of human parainfluenza virus type 3 yield viruses with temperature-sensitive and attenuation phenotypes. Virology **272:**225–234.
44. **Skiadopoulos, M. H., S. R. Surman, J. M. Riggs, C. Orvell, P. L. Collins, and B. R. Murphy.** 2002. Evaluation of the replication and immunogenicity of recombinant human parainfluenza virus type 3 vectors expressing up to 3 foreign glycoproteins. Virology 296.
45. **Sullivan, N. J., T. W. Geisbert, J. B. Geisbert, L. Xu, Z. Y. Yang, M. Roederer, R. A. Koup, P. B. Jahrling, and G. J. Nabel.** 2003. Accelerated

vaccination for Ebola virus haemorrhagic fever in non-human primates. Nature **424:**681–684.

46. **Sullivan, N. J., M. Peterson, Z. Y. Yang, W. P. Kong, H. Duckers, E. Nabel, and G. J. Nabel.** 2005. Ebola virus glycoprotein toxicity is mediated by a dynamin-dependent protein-trafficking pathway. J. Virol. **79:**547–553.
47. **Sullivan, N. J., A. Sanchez, P. E. Rollin, Z. Y. Yang, and G. J. Nabel.** 2000. Development of a preventive vaccine for Ebola virus infection in primates. Nature **408:**605–609.
48. **Teng, M. N., S. S. Whitehead, A. Bermingham, M. St Claire, W. R. Elkins, B. R. Murphy, and P. L. Collins.** 2000. Recombinant respiratory syncytial virus that does not express the NS1 or M2-2 protein is highly attenuated and immunogenic in chimpanzees. J. Virol. **74:**9317–9321.
49. **van Wyke Coelingh, K. L., C. Winter, and B. R. Murphy.** 1985. Antigenic variation in the hemagglutinin-neuraminidase protein of human parainfluenza type 3 virus. Virology **143:**569–582.
50. **Volchkov, V. E., S. Becker, V. A. Volchkova, V. A. Ternovoj, A. N. Kotov, S. V. Netesov, and H. D. Klenk.** 1995. GP mRNA of Ebola virus is edited by the Ebola virus polymerase and by T7 and vaccinia virus polymerases. Virology **214:**421–430.
51. **Volchkov, V. E., A. A. Chepurnov, V. A. Volchkova, V. A. Ternovoj, and H. D. Klenk.** 2000. Molecular characterization of guinea pig-adapted variants of Ebola virus. Virology **277:**147–155.
52. **Volchkov, V. E., H. Feldmann, V. A. Volchkova, and H. D. Klenk.** 1998. Processing of the Ebola virus glycoprotein by the proprotein convertase furin. Proc. Natl. Acad. Sci. USA **95:**5762–5767.
53. **Volchkov, V. E., V. A. Volchkova, E. Muhlberger, L. V. Kolesnikova, M. Weik, O. Dolnik, and H. D. Klenk.** 2001. Recovery of infectious Ebola virus from complementary DNA: RNA editing of the GP gene and viral cytotoxicity. Science **291:**1965–1969.
54. **Xu, L., A. Sanchez, Z. Yang, S. R. Zaki, E. G. Nabel, S. T. Nichol, and G. J. Nabel.** 1998. Immunization for Ebola virus infection. Nat. Med. **4:**37–42.
55. **Yang, Z. Y., H. J. Duckers, N. J. Sullivan, A. Sanchez, E. G. Nabel, and G. J. Nabel.** 2000. Identification of the Ebola virus glycoprotein as the main viral determinant of vascular cell cytotoxicity and injury. Nat. Med. **6:**886–889.
56. **Zaki, S. R., W. J. Shieh, P. W. Greer, C. S. Goldsmith, T. Ferebee, J. Katshitshi, F. K. Tshioko, M. A. Bwaka, R. Swanepoel, P. Calain, A. S. Khan, E. Lloyd, P. E. Rollin, T. G. Ksiazek, C. J. Peters, et al.** 1999. A novel immunohistochemical assay for the detection of Ebola virus in skin: implications for diagnosis, spread, and surveillance of Ebola hemorrhagic fever. J. Infect. Dis. **179**(Suppl. 1)**:**S36–S47.